Petroleum Coke on Hg^0 Removal

Subjects: Environmental Sciences

Contributor: Jie Jiang , Yongfa Diao

As the solid waste by-product from the delayed coking process, high-sulfur petroleum coke (HSPC), which is hardly used for green utilization, becomes a promising raw material for Hg^0 removal from coal-fired flue gas. The effects of the physical–chemical evolution of HSPC on Hg^0 removal are discussed. The improved micropores created by pyrolysis and KOH activation could lead to over 50% of Hg^0 removal efficiency with the loss of inherent sulfur. Additional S-containing and Br-containing additives are usually introduced to enhance active surface functional groups for Hg^0 oxidation, where the main product are HgS, HgBr, and HgBr$_2$. The chemical–mechanical activation method can make additives well loaded on the surface for Hg^0 removal.

high-sulfur petroleum coke   Hg0 removal

1. Introduction

As the solid waste by-product of the delayed coking process in the oil industry, petroleum cokes are utilized according to their sulfur-containing which are represented by low-sulfur petroleum coke (<3% S-containing) [1] and high-sulfur petroleum coke (>3% S-containing) [2]. Low-sulfur petroleum coke (LSPC) has maturely been used as anode raw material for electrolytic aluminum [3] and graphite electrodes [4] in steel plants, which accounts for 56.7% and 3.94%, respectively. By contrast, the proportion of fuel in cement plants and power plants using high-sulfur petroleum coke (HSPC) was just 6.19% [5]. Although the share of HSPC is not dominated, its absolute output is still high which was 1100 million tons in 2015, and maintains a fast-growing pace [6], especially in those countries which imported raw oil from the Middle East. Investigated from crude oil-producing areas, such as Saudi Arabia and Iran, the sulfur in raw oil is usually higher than 2.5% due to conventional plant remains during crude oil generation in these specific geographic locations. The pollutant represented by SO$_x$, which is released during the combustion of HSPC as fuel, has raised high concern for the atmospheric environment by global governments and organizations [7].

On the other hand, mercury also has caused global concern due to its high toxicity to the human body [8][9]. Mercury emissions are mainly derived from coal-fired plants which account for approximately 50% [10], especially in developing countries, such as China, which exist a high need for coal by 2018 [11]. The forms of the presence of mercury in the flue gas from coal-fired plants are the three, particulate-bound mercury (Hg^p), oxidized mercury (Hg^{2+}), and element mercury (Hg^0) [12]. The first two forms of mercury can be almost completely captured through fabric filters (FF) and wet flue gas desulfurization (WFGD) devices respectively due to those characteristics [13]. However, conventional desulfurization and dust removal equipment cannot succeed to achieve acceptable performance in the removal of element mercury [14]. Although elemental mercury emission is a trace from the coal-

fired industry, the accumulation and difficult removal properties, which are water-insoluble and volatile, have brought a worldwide threat to the biological environment and human health [15]. Therefore, compared to the high preparation cost of commercial activated carbon, which is usually modified by bromine [16], HSPC is a more attractive adsorbent for element mercury removal from coal-fired power plants due to its high sulfur-containing and also inexpensive cost. Furthermore, removing pollutants, which as the element mercury, with waste, which as HSPC, is the full use of artificial waste resources and meets the long-term requirements of carbon peaking and neutrality.
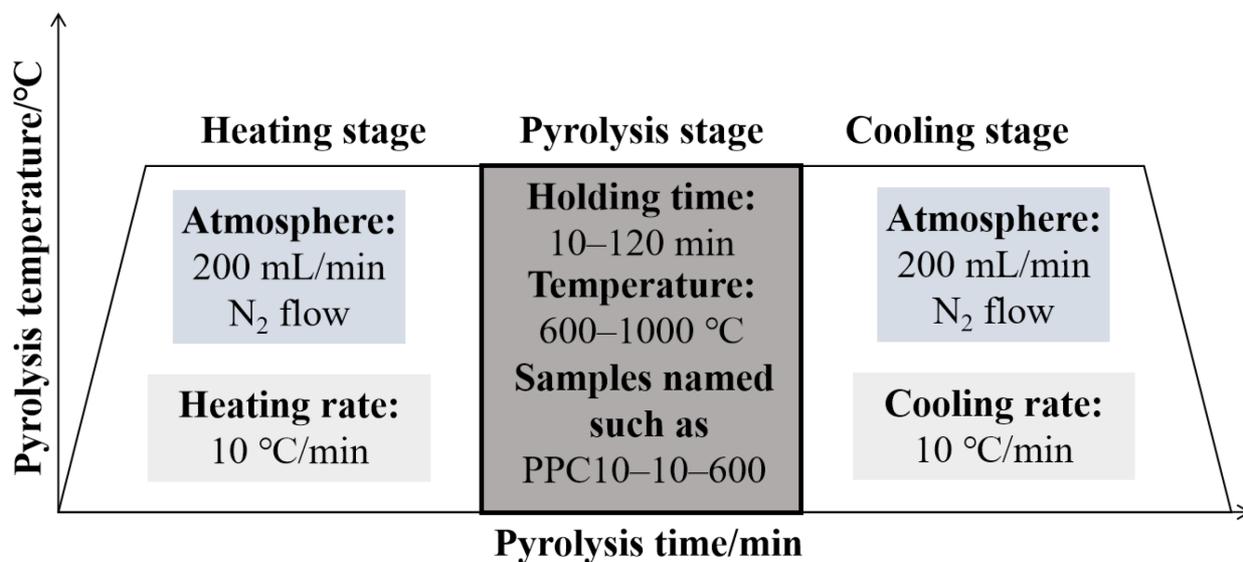
Compared to various raw materials for carbon-based activated adsorbents, such as fly ash [17][18], agricultural waste [19][20], and marine resources (sargassum and enteromorpha) [21], HSPC shows advantages as a promising candidate for its global production and relative stability of quality as low-economic-value waste. Furthermore, it is the sulfur in HSPC, which is the reason for the unsatisfactory selection as fuel, that is expected to oxidize Hg^0 to HgS which is recognized as the most environmentally friendly form of mercury oxide. Yang et al. [22] prepared a regenerable Co-MF catalyst based on fly ash for Hg^0 removal, where the catalyst played the oxidation role rather than the fly ash itself. Liu et al. [23] concluded that unburned carbon (UBC), Fe_2O_3, SiO_2, AlO_3, and CaO are the main reactive components in fly ash for Hg^0 oxidation. In terms of production, HgO, which is the main oxidation production, is formed by metal oxides as well as mental positive ions. However, HgO is not so stable at high heating temperatures. Thus, the bromination [17][24] impregnation method for fly ash activation was conducted and high removal efficiency (almost 100%) was achieved. However, the same problem occurs. The final production, which is $HgBr_2$, on the fly ash is readily volatile to air and leachable in water [25], which means secondary pollution during the coming disposal. For the raw materials of biomass, biomass-based activated carbon is usually prepared by improving pore structure, which is lacking for fly ash, and chemical activation. Thus, no matter which raw materials are used, chemical activation is the crucial activation process for element mercury removal, which plays a role in its oxidation and significantly improves its removal efficiency. The methods, including microwave activation, freeze-drying [26] and CO_2 activation [27], and KOH activation [28], are used to optimize the pore structure. Spessato et al. [28] successfully obtained the ideal BET surface of Jatoba's barks using KOH which were 2794 m^2/g and 889 m^2/g for SAC and RSAC, respectively. Apart from this, KOH activation during biomass pyrolysis [29] provided extra O-containing functional groups which benefit oxidizing element mercury. As such, the method combined KOH activation and pyrolysis seems an advanced activation technology for those materials which are expected to be porous for element mercury removal. Wu et al. [30] obtained a specific surface area of at most 3000 m^2/g, which came up with commercial activated carbon. The fresh high-sulfur petroleum coke, which contained 6.2% total sulfur, was activated using KOH by Zhu et al. [31]. Although the specific surface area reached 1713.8 m^2/g, the sulfur for element mercury oxidation almost lost and was not fully utilized. Therefore, this combined method is not a proper activation measure for HSPC due to its resource-wasting actions. Nonetheless, the actual ideal pore structure of petroleum coke has been a rare quantitative study for element mercury removal, including the parameters of particle size, specific surface area, and pore diameter as well as its shape. Due to the lack of sulfur which is in the favor of mercury, extra additives, such as SO_2 [32] and NH_4Br [33], for activation are needed to improve Hg^0 removal performance. In comparison, HSPC has an outlook of few additives for activation due to sulfur-containing itself. Furthermore, mechanochemical modification is also used in the preparation of adsorbents

for raw petroleum coke [34] because it is a simple operation process and ecologically safe [35]. This activation method should conduct more experimental exploration and mechanism research to adapt the directional preparation of HSPC. Meanwhile, the basic understanding of mechanisms of related modified activation and mercury removal using modified HSPC needs further studies which are the foundation for both pilot experiments and actual application.

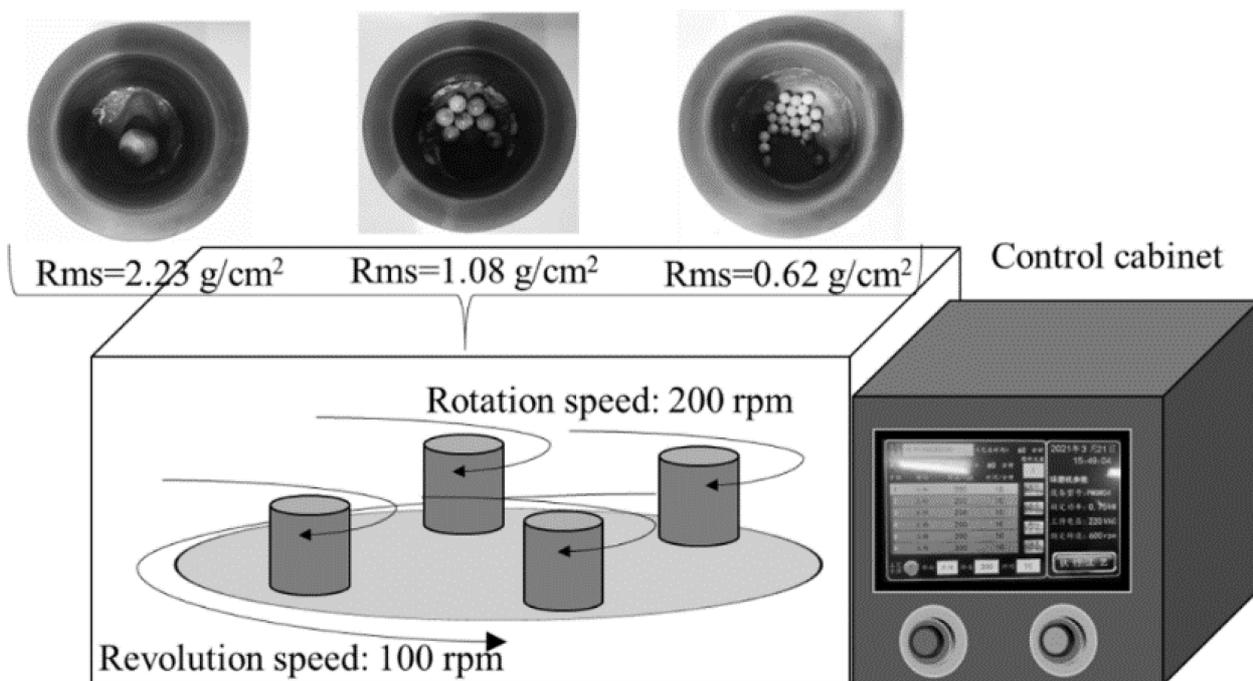## 2. The Effect of the Evolution of Pore Structure on Hg^0 Removal

The pore structure of raw HSPC is identified as poor for Hg^0 adsorption due to its dense structure. In particular, the Brunauer–Emmett–Teller (BET) surface area of raw HSPC is tested to be less than 1.1 m^2/g [36] and the total pore volume is almost zero [37]. It is the reason for the poor performance of pore structure on Hg^0 adsorption and also the lack of positions for active sites. The current modification process to active petroleum coke, including only or combined chemical, pyrolysis, mechanochemistry, and KOH activation, almost improved the pore structure of HSPC to a certain extent.

For only chemical activation, Xiao et al. [38] used a chemical–mechanical bromination process [39] for brominating the petroleum coke sample, as shown in **Figure 1**c. Although the mechanical impregnation method presented well bromine loading, both specific surface area and average pore size were slightly reduced to 1.66 m^2/g and 0.012 cm^3/g, which was caused by the blockage of pores during the bromination process. It is believed that external mechanical force caused by grinding could not promote the development of rich pores. While this bromination method made an excellent performance of Hg^0 removal, it was almost owing to the chemically loaded bromine of C-Br rather than the contribution of pore structure.

Heating stage

Atmosphere:
200 mL/min
N_2 flow

Heating rate:
10 °C/min

Pyrolysis stage

Holding time:
10–120 min
Temperature:
600–1000 °C
Samples named
such as
PPC10–10–600

Cooling stage

Atmosphere:
200 mL/min
N_2 flow

Cooling rate:
10 °C/min

(a)

Different diameter of grinding ball in the same ball mill tank

Rms=2.23 g/cm^2 Rms=1.08 g/cm^2 Rms=0.62 g/cm^2

Control cabinet

Rotation speed: 200 rpm

Revolution speed: 100 rpm

Omni-Directional Planetary Ball Mill
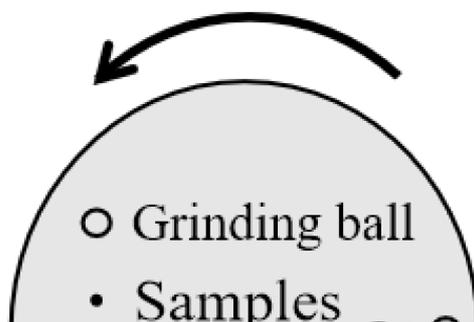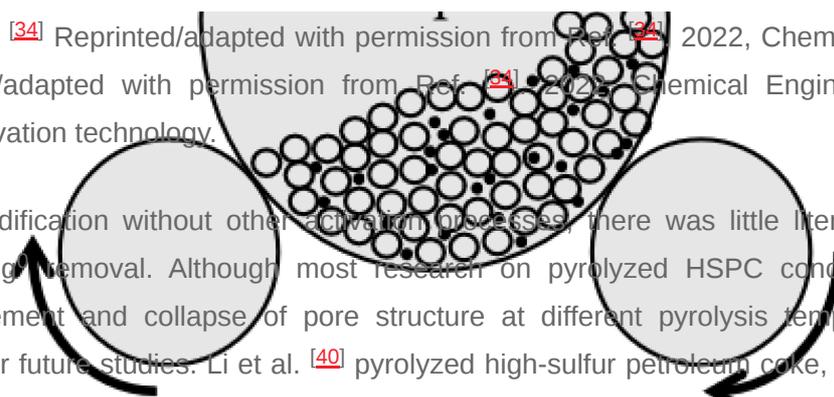
(b)

○ Grinding ball
• Samples

Figure 1. (**a**) Pyrolysis [34] Reprinted/adapted with permission from Ref. [34], 2022, Chemical Engineering Journal; (**b**) 1st [34] Reprinted/adapted with permission from Ref. [34], 2022, Chemical Engineering Journal; (**c**) 2nd mechanochemical activation technology.

For only pyrolysis modification without other activation processes, there was little literature on only pyrolyzed petroleum coke for Hg removal. Although most research on pyrolyzed HSPC concentrated on gasification reactivity, the improvement and collapse of pore structure at different pyrolysis temperatures would provide valuable information for future studies. Li et al. [40] pyrolyzed high-sulfur petroleum coke, which was sieved to 83–165 μm, at the final temperature of 1223, 1473, and 1673 K with a pyrolysis heating rate of 10 K/min and holding time of 30 min under the atmosphere of N$_2$. The test results showed that the BET surface area of the pyrolyzed samples was 15.62, 28.52, and 3.03 m^2/g. The same trend occurred in the total pore volume that the smallest one was 0.0085 cm^3/g and lower than half of that at 1473 K. The reason for it was the ash was melted at this high temperature and the melt blocked the micropore. Hence, excessive pyrolysis temperature was not conducive to the formation of an extremely rich pore structure. Lee et al. [36] divided the pyrolyzed PC, which was heated up to 1100 °C under N$_2$ within 30 min, by the particle size of 200, 400, and 500 mesh. The results showed that the smaller particle size led to the larger specific surface area where the largest one was 11.7 m^2/g. Compared to other activated carbon (AC) with a specific surface area of more than 1000 m^2/g, such as HGR, SH-S, and Norit GL, PC-400 had a promising Hg^0 removal performance while its specific surface area was only 1/100 of that of these three commercial AC. This work concluded that the reason was that mesopores above 50 Å were developed for the PC400 after pyrolysis and sulfur separated from carbon and adhered to macropores in the process of PC pyrolysis. On the contrary, the quantity of sulfur adhered to the micro-pores was smaller than that in the macro-pores. It should be noted that the formation of pores in commercial AC is almost that of micropores. Hence, although the chemical oxidation offers a more active and stable fix for Hg^0, the advanced pore structure with different proportions of macropores, mesopores, and micropores should be explored.

For the combined pyrolysis and mechanochemistry activation method, Ma et al. [34] crushed the samples with particle sizes lower than 100 mesh and carried on the only pyrolysis (**Figure 1**a), mechanochemical activation (**Figure 1**b), and the combined pyrolysis and mechanochemical activation experiments. The final temperature and holding time of pyrolysis parameters were concerned. The omni-directional planetary ball mill was selected for mechanochemical activation, which was the same method as Xiao et al. [38] with different equipment. It was observed that the largest specific area of 31.77 m^2/g, the total pore volume of 0.027 cm^3/g, and the smallest mean pore diameter of 3.39 nm occurred in PPC10-60-800. The influence of final pyrolysis temperatures was the collapse of pore structure happened at 900 °C, which was approximately lower than 200 °C compared to other experiments. In terms of only mechanochemical activation, the largest specific surface area reached 5.93 m^2/g and the mean pore diameter came to 8.1 nm. However, its development was not considerable as that of pyrolysis. Combined with the results of Xiao et al. [38], it can be concluded that the significant contribution of mechanochemical activation is mainly for the chemical loading rather than the improvement of pore structure. The mercury removal efficiency of only pyrolysis, only mechanochemical activation, and the combined pyrolysis and mechanochemical activation were 29.15%, 25.68%, and 27.8%, respectively, which indicated that the improved pore structure could act as conventional functional groups, such as C–O, C–O–C, and C=O, for mercury removal.

Hence, the optimal pore structure can improve the mercury removal performance of HSPC to a certain extent which cannot be vague and random identification. It is noted that pyrolysis parameters are raised concern for the development of optimal pore structure for Hg[0] adsorption and better chemical loading for Hg[0] oxidation, such as atmosphere, final temperature, heating, and cooling rate, holding time, and even the mesh selection for controllable pyrolysis. Zhao et al. [41] reported the largest specific surface area of pyrolyzed biomass coke by pyrolysis parameters of 7% O_2, 800 °C, and the heating rate of 10 K/min. Moreover, the micropore structure was obtained with an average pore diameter of 1.93 nm. Therefore, sufficient attempts and explorations of pyrolysis parameters should be conducted in the future.

For the combined pyrolysis and chemical activation method, Huo et al. [37] prepared AC from HSPC with zinc nitrate in the following process, 2 h ultrasound mixing, 12 h dry at 60 °C, 5 h calcine, and physical activation at high temperature. The specific surface area of the ZnS/AC sample was 0.21 m^2/g, which also indicated that chemical activation could not well improve the pore structure [38]. The activation parameters that 950 °C, 40 vol% water stream, and 2.5 h activation time were selected. Then, the optimal specific surface area, total pore volume, and average pore diameter were obtained, which were 235.84 m^2/g, 0.139 cm^3/g, and 3.9 nm, respectively. The comparisons of four samples on Hg[0] removal before and after these two activation process were given (**Figure 2**). Apparently, Zn3/S10-A sample had the excellent Hg[0] performance at begin, and then decrease to 65% within 2 h, which is due to the developed pore structure and ZnS as active sites to oxidation Hg[0]. The Zn0/S10-A sample also showed a much higher Hg[0] removal efficiency compared to the other two samples without improved pore structure. This work further explained the reason for the decline of the Hg[0] removal efficiency of Zn0/S10-A, which is the consumption of a small part of released sulfur during pyrolysis. However, the specific contribution between pore structure and the active sites were not be mentioned. In other words, it is vague to distinguish these two contributions for Hg[0] removal and also identify their interaction. In addition, although the ZnS could not improve the pore structure, Hong et al. [42] pointed out the specific surface area of AC was developed up to 1475 m^2/g by $ZnCl_2$. The huge difference in the hole-enlarging effect of zinc-based additives may be the final pyrolysis temperature, which was due to the decomposition and vigorous movement of zinc-based additives at higher temperature (>500 °C). Meanwhile, the collapse of the pore structure was also 900 °C which was the same as Ma et al. [34]. It is noted that the $ZnCl_2$ activator has the potential to produce mesoporous AC [43], while some other activators such as KOH, NaOH, and Na_2CO_3 are beneficial to the production of microporous AC [44]. Thus, the mesoporous rate of samples activated by $ZnCl_2$ is high, reaching approximately 75%. It is assumed that a rich mesoporous structure might better promote further chemical loading than a microporous structure. In addition, the preparation mechanism by $ZnCl_2$ was proposed [42] (Equations (1) and (2)).
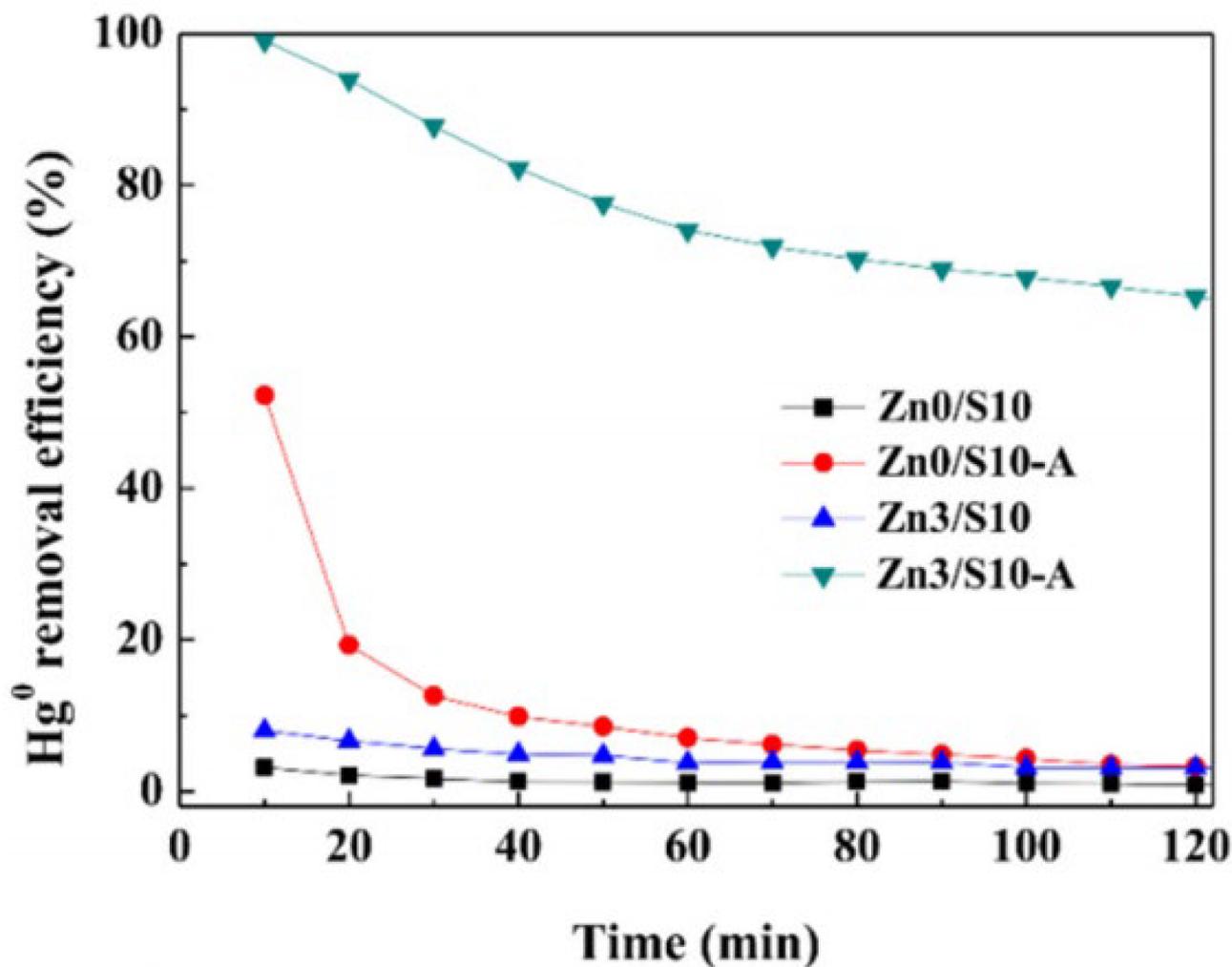
Figure 2. Hg^0 removal performance of different ZnS sorbents at different temperatures [37]. Reprinted/adapted with permission from Ref. [37]. 2019, Fuel Processing Technology.

References

1. Wang, M.; Wan, Y.; Guo, Q.; Bai, Y.; Yu, G.; Liu, Y.; Zhang, H.; Zhang, S.; Wei, J. Brief review on petroleum coke and biomass/coal co-gasification: Syngas production, reactivity characteristics, and synergy behavior. Fuel 2021, 304, 121517.

2. Cai, W.; Li, K.; Jiang, K.; Lv, D.; Liu, Y.-Q.; Wang, D.; Wang, X.; Lai, C. Utilization of high-sulfur-containing petroleum coke for making sulfur-doped porous carbon composite material and its application in supercapacitors. Diam. Relat. Mater. 2021, 116, 108380.

3. Tyutrin, A.A.; Burdonov, A.E.; Bushuev, K.S. Expanding the Application Scope of Fine Dust from Petroleum Coke Calcining Furnaces in Aluminum Production. Mater. Sci. Forum 2022, 1052, 482–487.

4. Veluri, P.S.; Katchala, N.; Anandan, S.; Pramanik, M.; NarayanSrinivasan, K.; Ravi, B.; Rao, N.T. Petroleum Coke as an Efficient Single Carbon Source for High-Energy and High-Power Lithium-Ion Capacitors. Energy Fuels 2021, 35, 9010–9016.

5. Liu, L.; Li, Z.; Wu, S.; Li, D.; Cai, N. Conversion characteristics of lignite and petroleum coke in chemical looping combustion coupled with an annular carbon stripper. Fuel Process. Technol. 2021, 213, 106711.

6. Shan, Y.; Guan, D.; Meng, J.; Liu, Z.; Schroeder, H.; Liu, J.; Mi, Z. Rapid growth of petroleum coke consumption and its related emissions in China. Appl. Energy 2018, 226, 494–502.

7. Andrews, A.; Lattanzio, R.K. Petroleum Coke: Industry and Environmental Issues; Congressional Research Service: Washington DC, USA, 2013.

8. Mackey, T.K.; Contreras, J.T.; Liang, B.A. The Minamata Convention on Mercury: Attempting to address the global controversy of dental amalgam use and mercury waste disposal. Sci. Total Environ. 2014, 472, 125–129.

9. Wang, L.; Hou, D.; Cao, Y.; Ok, Y.S.; Tack, F.M.; Rinklebe, J.; O'Connor, D. Remediation of mercury contaminated soil, water, and air: A review of emerging materials and innovative technologies. Environ. Int. 2020, 134, 105281.

10. Streets, D.G.; Devane, M.K.; Lu, Z.; Bond, T.C.; Sunderland, E.M.; Jacob, D.J. All-time releases of mercury to the atmosphere from human activities. Environ. Sci. Technol. 2011, 45, 10485–10491.

11. Liu, K.; Wang, S.; Wu, Q.; Wang, L.; Ma, Q.; Zhang, L.; Li, G.; Tian, H.; Duan, L.; Hao, J. A highly resolved mercury emission inventory of Chinese coal-fired power plants. Environ. Sci. Technol. 2018, 52, 2400–2408.

12. Zhao, S.; Pudasainee, D.; Duan, Y.; Gupta, R.; Liu, M.; Lu, J. A review on mercury in coal combustion process: Content and occurrence forms in coal, transformation, sampling methods, emission and control technologies. Prog. Energy Combust. Sci. 2019, 73, 26–64.

13. Li, Y.; Yu, J.; Liu, Y.; Huang, R.; Wang, Z.; Zhao, Y. A Review on Removal of Mercury from Flue Gas Utilizing Existing Air Pollutant Control Devices (APCDs). J. Hazard. Mater. 2022, 427, 128132.

14. Li, G.; Wu, Q.; Xu, L.; Wen, M.; Liu, K.; Tang, Y.; Zou, J.; Wang, F.; Wang, Y.; Wang, S. A review on adsorption technologies for mercury emission control. Bull. Environ. Contam. Toxicol. 2019, 103, 155–162.

15. Beckers, F.; Rinklebe, J. Cycling of mercury in the environment: Sources, fate, and human health implications: A review. Crit. Rev. Environ. Sci. Technol. 2017, 47, 693–794.

16. Sasmaz, E.; Kirchofer, A.; Jew, A.D.; Saha, A.; Abram, D.; Jaramillo, T.F.; Wilcox, J. Mercury chemistry on brominated activated carbon. Fuel 2012, 99, 188–196.

17. Hu, J.; Geng, X.; Duan, Y.; Zhao, W.; Zhu, M.; Ren, S. Effect of mechanical–chemical modification process on mercury removal of bromine modified fly ash. Energy Fuels 2020, 34, 9829–9839.

18. Ochedi, F.O.; Liu, Y.; Hussain, A. A review on coal fly ash-based adsorbents for mercury and arsenic removal. J. Clean. Prod. 2020, 267, 122143.

19. Zhu, C.; Duan, Y.; Wu, C.-Y.; Zhou, Q.; She, M.; Yao, T.; Zhang, J. Mercury removal and synergistic capture of SO2/NO by ammonium halides modified rice husk char. Fuel 2016, 172, 160–169.

20. Zafari, R. Synthesis and Study of Modified-Nanocrystalline Cellulose Effective for SO2 Capture; University of Ottawa: Ottawa, ON, Canada, 2021.

21. Liu, Z.; Adewuyi, Y.G.; Shi, S.; Chen, H.; Li, Y.; Liu, D.; Liu, Y. Removal of gaseous Hg0 using novel seaweed biomass-based activated carbon. Chem. Eng. J. 2019, 366, 41–49.

22. Yang, J.; Zhao, Y.; Zhang, J.; Zheng, C. Regenerable cobalt oxide loaded magnetosphere catalyst from fly ash for mercury removal in coal combustion flue gas. Env. Sci. Technol. 2014, 48, 14837–14843.

23. Liu, Z.; Liu, D.; Zhao, B.; Feng, L.; Ni, M.; Jin, J. Mercury Removal Based on Adsorption and Oxidation by Fly Ash: A Review. Energy Fuels 2020, 34, 11840–11866.

24. Wang, S.; Zhang, Y.; Gu, Y.; Wang, J.; Yu, X.; Wang, T.; Sun, Z.; Romero, C.E.; Pan, W.-p. Coupling of bromide and on-line mechanical modified fly ash for mercury removal at a 1000 MW coal-fired power plant. Fuel 2019, 247, 179–186.

25. Graydon, J.W.; Zhang, X.; Kirk, D.W.; Jia, C.Q. Sorption and stability of mercury on activated carbon for emission control. J. Hazard. Mater. 2009, 168, 978–982.

26. Yang, W.; Li, Y.; Shi, S.; Chen, H.; Shan, Y.; Liu, Y. Mercury removal from flue gas by magnetic iron-copper oxide modified porous char derived from biomass materials. Fuel 2019, 256, 115977.

27. Shen, F.; Liu, J.; Dong, Y.; Wu, D. Mercury removal by biomass-derived porous carbon: Experimental and theoretical insights into the effect of H2S. Chem. Eng. J. 2018, 348, 409–415.

28. Spessato, L.; Bedin, K.C.; Cazetta, A.L.; Souza, I.P.; Duarte, V.A.; Crespo, L.H.; Silva, M.C.; Pontes, R.M.; Almeida, V.C. KOH-super activated carbon from biomass waste: Insights into the paracetamol adsorption mechanism and thermal regeneration cycles. J. Hazard. Mater. 2019, 371, 499–505.

29. Chen, W.; Gong, M.; Li, K.; Xia, M.; Chen, Z.; Xiao, H.; Fang, Y.; Chen, Y.; Yang, H.; Chen, H. Insight into KOH activation mechanism during biomass pyrolysis: Chemical reactions between O-containing groups and KOH. Appl. Energy 2020, 278, 115730.

30. Wu, M.B.; Zha, Q.F.; Qiu, J.S.; Han, X.; Guo, Y.S.; Li, Z.F.; Yuan, A.J.; Sun, X. Preparation of porous carbons from petroleum coke by different activation methods. Fuel 2005, 84, 1992–1997.

31. Zhu, M.; Yan, Q.; Duan, Y.; Li, J.; Zhang, X.; Han, Z.; Meng, J.; Wang, S.; Chen, C.; Wei, H. Study on Preparation and Mercury Adsorption Characteristics of Columnar Sulfur-Impregnated Activated Petroleum Coke. Energy Fuels 2020, 34, 10740–10751.

32. She, M.; Jia, C.Q.; Duan, Y.; Zhu, C. Influence of Different Sulfur Forms on Gas-Phase Mercury Removal by SO2-Impregnated Porous Carbons. Energy Fuels 2020, 34, 2064–2073.

33. Shen, C.; Wang, H.; Shen, H.; Wu, J.; Zhu, Y.; Shi, W.; Zhang, X.; Ying, Z. NH4Br-Modified Biomass Char for Mercury Removal in a Simulated Oxy-fuel Atmosphere: Mechanism Analysis by X-ray Photoelectron Spectroscopy. Energy Fuels 2020, 34, 9872–9884.

34. Ma, A.; Zhao, S.; Luo, H.; Sun, Z.; Xie, X.; Liao, Y.; Liang, X.; Li, H. Mercury removal from coal-fired flue gas of high-sulfur petroleum coke activated by pyrolysis and mechanochemical method. Chem. Eng. J. 2022, 429, 132154.

35. Sun, Z.; Ma, A.; Zhao, S.; Luo, H.; Xie, X.; Liao, Y.; Liang, X. Research progress on petroleum coke for mercury removal from coal-fired flue gas. Fuel 2022, 309, 122084.

36. Lee, S.H.; Rhim, Y.J.; Cho, S.P.; Baek, J.I. Carbon-based novel sorbent for removing gas-phase mercury. Fuel 2006, 85, 219–226.

37. Huo, Q.; Wang, Y.; Chen, H.; Han, L.; Wang, J.; Bao, W.; Chang, L.; Xie, K. ZnS/AC sorbent derived from the high sulfur petroleum coke for mercury removal. Fuel Process. Technol. 2019, 191, 36–43.

38. Xiao, Y.; Pudasainee, D.; Gupta, R.; Xu, Z.; Diao, Y. Bromination of petroleum coke for elemental mercury capture. J. Hazard. Mater. 2017, 336, 232–239.

39. Fuente-Cuesta, A.; Diaz-Somoano, M.; Lopez-Anton, M.; Cieplik, M.; Fierro, J.; Martínez-Tarazona, M. Biomass gasification chars for mercury capture from a simulated flue gas of coal combustion. J. Environ. Manag. 2012, 98, 23–28.

40. Li, C.; Liu, X.; Zhou, Z.; Dai, Z.; Yang, J.; Wang, F. Effect of heat treatment on structure and gasification reactivity of petroleum coke. Int. J. Coal Sci. Technol. 2016, 3, 53–61.

41. Zhao, S.; Luo, H.; Ma, A.; Xie, W.; Sun, K.; Sun, Z. Influence of pyrolysis conditions on the mercury removal characteristics and physicochemical properties of biomass coke. Fuel 2022, 313, 122979.

42. Hong, D.; Zhou, J.; Hu, C.; Zhou, Q.; Mao, J.; Qin, Q. Mercury removal mechanism of AC prepared by one-step activation with ZnCl2. Fuel 2019, 235, 326–335.

43. Zhao, J.; Dai, Y.; Xu, J.; Chen, S.; Xie, J. Synthesis and electrochemical characterization of mesoporous carbons prepared by chemical activation. J. Electrochem. Soc. 2008, 155, A475.

44. Adinata, D.; Daud, W.M.A.W.; Aroua, M.K. Preparation and characterization of activated carbon from palm shell by chemical activation with K2CO3. Bioresour. Technol. 2007, 98, 145–149.

Retrieved from https://encyclopedia.pub/entry/history/show/57878